Decreased Expression of ENPP6 Predicts the Occurrence of Pain in Malignant Spinal Tumour

Jie Hu

The First Affiliated Hospital of Xi'an Jiaotong University

Birou Zhong

Chongqing Medical University

Yuqian Guo (✉ 2018110118@stu.cqmu.edu.cn)

Chongqing Medical University   https://orcid.org/0000-0001-7968-9370

Primary research

Abstract

Background: Neuropathic pain (NeP) characterized by neuroplasticity and neuroinflammatory change is a common complication associated with spinal metastasis. However, there are no reliable candidates for diagnosis and treatment. Recently, cancer research has incorporated molecules into the treatment of patients with NeP, therefore, it is necessary to find key molecules of NeP to provide new targets for diagnosis and treatment.

Methods: We analyzed RNA-seq data around the expression of ENPP6 based on bioinformatic methods, including differentially expressed genes (DEGs), Gene Ontology (GO), protein-protein interaction (PPI) network, Kyoto Encyclopedia of Genes and Genomes (KEGG) and GSEA analyses, receiver operating characteristic (ROC) curve, immune cell infiltration and mutation analysis.

Results: We divided with pain samples into the High and Low ENPP6 expression groups. A total of 231 DEGs were identified. GO and KEGG analysis showed that DEGs were mainly enriched in Inflammation and cancer associated pathways. GSEA analysis showed that DEGs was significantly enriched in ARF3 and P38/MK2, RHO and RAS, and BRAFT and AKT1/E17K pathway. Pearson's correlation analysis showed that the expression of ENPP6 was significantly correlated with autophagy phenotype and immunophenotype. Immune infiltrating analysis showed that activated NK cells were significantly highly expressed in Low group. ROC analysis of ENPP6 suggested that the area under the ROC curve was 0.925. Mutation sites analysis showed that most of the mutations in ENPP4-7 were phosphorylation sites.

Conclusion: This study provides novel insights into molecular mechanisms underlying NeP, and identifying ENPP6 may serve as potentially diagnostic biomarkers and/or therapeutic targets for NeP.

1 Introduction

Chronic pain has been estimated to affect one-sixth of the population[1]. Cancer-related neuropathic pain (NeP) is a neuroplasticity and neuroinflammatory change caused by damage to the somatosensory system caused by treatment, cancer or paraneoplastic reactions to cancer[2, 3]. Spine is a common organ for metastatic cancer, and in patients with advanced cancer, spinal metastasis can lead to significant pain or neurological dysfunction, which impacting the quality of life[4, 5]. Although advanced radiotherapy and surgical techniques are available for patients with advanced spinal metastases[6, 7], some of them have a persistent pain during or shortly after radiotherapy and surgery treatment[8]. Current targeted drugs have many limitations, such as unsatisfactory efficacy and uncontrollable dosage. And few studies have focused on the diagnosis and treatment of patients with cancer-related NeP[2]. Notably, cancer research nowadays has incorporated a variety of molecules into the treatment of cancer patients with NeP, therefore, it is necessary to find key molecules of NeP to provide new targets for diagnosis and treatment.

Ectonucleotide Pyrophosphatase/Phosphodiesterase6 (ENPP6, ENSP00000296741), which belongs to ENPP family, comprising seven members with structurally related catalytic domains[9]. ENPP1–3 are type

II transmembrane proteins, which consist of catalytic domains and nuclease-like domain. ENPP4–7 are type I membrane proteins, which consist of catalytic domains only[10]. ENPP6 is a plasma membrane associated or secreted ectoenzyme that can hydrolyze glycerophosphocholine (GPC) and lysophosphatidylcholine (LPC) and contributes to supplying choline to the cells [11, 12]. In mice, ENPP6 mRNA was primarily detected in kidney and brain with a lesser expression in heart[13], and in human it was detected in kidney, ovary and brain[11, 14]. Recent research shows that ENPP6 may play a critical role in diseases of the bone, nervous system and cancer[15–18].

The management of NeP in malignant spinal tumour is extremely complex, so its treatment still faces great challenges. Many promising treatments found in animal models have failed in clinical trials, possibly because of basic cellular and molecular differences between animals and humans[19, 20]. It may be possible to identify new drug targets by screening and analyzing the human gene networks associated with pain formation and progression. There has been no report about the correlation between ENPP6 and NeP in patients with cancer. Therefore, this study aims to analyze human RNA-seq data from PAIN Neurobiology Research Group using bioinformatics methods to explore the potential value of ENPP6 in the diagnosis and treatment of patients with spinal tumour.

2 Materials & Methods

2.1 Data of Patients and Treatment

Datasets and corresponding clinical information were collected of 15 patients undergoing treatment at MD Anderson Cancer Center for malignant tumour involving the spine. The data collection and this study were conducted in compliance with all applicable laws, regulations and policies for the protection of human subjects, and any necessary approvals, authorizations, human subject assurances, informed consent documents[21]. The data type was RNA-seq, and the tissue sample was human dorsal root ganglion (DRG) neuron. This study included 21 samples which from 15 patients, including $n = 16$ with pain samples (P) ($n = 7$, 1–6 months; $n = 4$, 6–12 months; $n = 5$, > 12 months) and $n = 5$ no pain samples (NP). Randomly divided $n = 16$ with pain samples into two groups (P1, P2), and made sure that the samples in each group were from different patients. Each with pain group was compared separately with the no pain group, then a cross validation for each group were performed.

2.2 RNA-sequencing data and bioinformatics analysis

Gene expression data were downloaded from PAIN Neurobiology Research Group(https://www.utdallas.edu/bbs/painneurosciencelab/sensoryomics/hdrgclinical/) (15 patients; 21 samples; tissue sample, human dorsal root ganglion neuron; data type, RNA-seq; workflow type, TPM). Then, the transcripts per million (TPM) data for 21 samples were used for the following analyses.

2.3 Screening Differential and Co-expression Gene.

These raw data already been background corrected and normalized. According to the median value of ENPP6 (TPM = 6.82), the 16 with pain samples were divided into the high (> 6.82; $n = 8$) and low (≤ 6.82;

n = 8) ENPP6 expression groups. Differentially expressed genes (DEGs) and co-expression gene were screened using the R package DEseq[22] and limma[23], according to the fold change (FC) and significant difference (*p* value) between groups. The threshold was set at delta = 1, log$_2$FC > 0.5) and *p* value < 0.05, then we obtained 231 DEGs. Next, volcano plots and heatmaps of differential gene were performed using R package, ggplot2 and pheatmap.

2.4 Human Protein Atlas

The Human Protein Atlas (HPA, https://www.proteinatlas.org/) is a database with the aim to map all the human proteins in cells, tissues and organs using an integration of various omics technologies, including antibody-based imaging, mass spectrometry-based proteomics, transcriptomics and systems biology. HPA consists of six separate parts (Tissue, Single Cell Type, Pathology, Blood, Brain, Cell). We obtained the expression analysis and Immunohistochemical (IHC) images of ENPP6 from the Tissue, Pathology, Blood and Brain Atlas.

2.5 GO Enrichment and KEGG Pathway Analysis.

DAVID[24, 25] was used for GO analysis of DEGs, which threshold was set at FDR < 0.1, then the visualization of results was performed using the ggplot2 R package. For Kyoto Encyclopedia of Genes and Genomes (KEGG) pathway enrichment analysis, we used the clusterProfiler package[26] and KEGG Orthology Based Annotation System 3.0 (KOBAS 3.0, http://kobas.cbi.pku.edu.cn) with *p* < 0.05 were considered to be significantly enriched, then produced the relevant bubble and bar charts.

2.6 Gene set enrichment analysis

Gene Set Enrichment Analysis (GSEA, version 4.0.3)[27] was used to analyze the DEGs matrix between ENPP6 high and low expression group, with the reference gene set (c2.cp.v7.0.symbols.gmt) and significance threshold of *p* < 0.05. Then, we use the RColorBrewer package for the visualization.

2.7 protein-protein interaction (PPI) network

STRING database[28] was used to construct the PPI network of DEGs, with the interaction score was set to confidence of 0.4, and the organism was set to 'Homo sapiens'. Currently, this database contains 18,838 proteins and 25,914,693 core interactions network. After construction of the PPI network, we use MCODE (MCODE scores > 5, node score cut-off = 0.2, degree cut-off = 2, Max depth = 100, and k-score = 2) and cytoHubba in Cytoscape to perform key sub-module analysis to obtain Hub genes and sub-modules with biological significance.

2.8 Phenotypic correlation analysis

The Human Autophagy Database (HADb) is the first dedicated human autophagy database, a common repository containing information about human genes related to autophagy described to date. We have acquired autophagy related genes list from the Hadb (http://www.autophagy.lu/index.html) and immune related genes list from the Immunology Database and Analysis Portal Database (ImmPort, https://immport.niaid.nih.gov/home). Subsequently, 12 genes were obtained by intersected with

autophagy/immune-related genes respectively for the 231 DEGs. Then, the 'plot' function in R was used to analyze the expression correlation between ENPP6 and the 12 genes, and visualized the results with significantly correlated.

2.9 CIBERSORT and LM22

CIBERSORT[29] is an analytical tool widely used to characterize the immune cell composition by gene expression values in tumors. LM22 signature matrix is a special genetic marker containing 547 genes that distinguish the 22 immune cell subtypes downloaded from the CIBERSORT (http://cibersort.stanford.edu/). In this study, CIBERSORT package and LM22 algorithm was used to analyze the abundance and expression divergence of 22 kinds of immune cells infiltrates between the groups with high and low ENPP6 expression in 16 pain samples.

2.10 Area Under the ROC Curve

Receiver operating characteristic (ROC) curve, which takes true (sensitivity) and false (1-specificity) positive rate as ordinate and abscissa respectively, R package "pROC" was applied to the analysis whether the expression of ENPP6 can distinguish with or without pain in 21 cases of samples, and determine the highest likelihood ratio of the optimal cut-off value to judge ENPP6 recognition threshold of pain. Area Under the ROC Curve (AUC) reflects the diagnostic value of biomarkers for diseases. In the case of AUC > 0.5, the closer the AUC to 1, the better the authenticity of diagnostic is.

2.11 Gene expression and mutations

The gene list of ENPP family members was obtained by using HUGO Gene Nomenclature Committee (HGNC) database[30]. Then we analyzed the mutations of ENPP family members in 32 TCGA pan-cancer data sets using the cBioPortal database. cBioPortal database is an open-source and open-data resource for interactive exploration of multiple cancer genomics database.

2.12 Statistical analysis

Data analysis was performed using R statistical software (version 4.0.2), and $p < 0.05$ was considered statistically significant.

3 Results

3.1 Downregulation of ENPP6 in malignant tumors of the spine patients with pain

To explore the expression of ENPP6 in pain patients with malignant tumors of the spine in dorsal root ganglion tissues, we first analyzed previously published datasets[21], including 21 ($n = 16$ with pain samples (P) and $n = 5$ no pain samples (NP)) samples of DRG from 15 patients which clinical features were summarized in Supplementary Table 1. Results showed that the expression of ENPP6 in pain group

was significantly lower than that in no pain group (Fig. 1. A, $p = 0.003$). However, there was no significant difference in other members of the ENPP family when compared the pain and no pain groups (Supplementary material Fig. 1).

3.2 Identification of DEGs in differential ENPP6 expression groups

After screened co-expressed genes by R package DEseq and limma (adjusted $log_2FC > 0.5$ and p value < 0.05), 231 differentially expressed genes were obtained, Including 216 upregulated and 15 downregulated genes. The volcano plot was used to represent the DEGs (Fig. 1. B), Subsequently, according to the median value of ENPP6 (TPM = 6.82), we divided 16 with pain samples into the high (H, > 6.82; $n = 8$) and low (L, ≤ 6.82; $n = 8$) ENPP6 expression groups. The heatmap was used to represent the distribution of the differential genes in the two groups with different ENPP6 expressions (Fig. 1. C).

3.3 Expression of ENPP6 in human brain

In the HPA database, we found that ENPP6 was highly expressed in the human brain, kidney and reproductive system (Fig. 2. A, B). It was also highly expressed in immune cells such as basophil and NK-cells (Fig. 2. D). However, the expression of ENPP6 was decreased in glioma (Fig. 2. C), and the cerebral cortex and tumour immunohistochemical comparison was shown (Fig. 2. E).

3.4 GO and KEGG pathway analyses correlated with DEGs

Using DAVID database, a total of 231 DEGs were subsequently applied to conduct GO and KEGG pathway enrichment analysis. In the "biological process" category, 47 enriched GO terms were observed. Categorization by "cellular component" revealed 21 enriched GO terms, such as neuronal cell body, endosome membrane and postsynaptic density. Moreover, the "molecular function" category revealed 19 significant enrichment, such as DNA – binding transcription factor binding, transcription corepressor activity, protein serine/threonine kinase activity. The details of the GO entries were described in Table 1. Results from GO enrichment analysis indicated that the DEGs were existed in endosome membrane of neuronal cell and were primarily associated with the immunoinflammation-related and regulation of trans-synaptic signaling GO terms, such as response to lipopolysaccharide, mononuclear cell migration, Ras protein signal transduction, modulation of chemical synaptic transmission and positive regulation of neurogenesis (Fig. 3. A-B). To reflect the internal interactions between these GO items, we constructed the GO interaction network as shown in Fig. 3. C-D.

Table 1
GO enrichment analysis of DEG between high and low ENPP6 expression groups

Ontology	ID(GO)	Count	P. adjust	Description
BP	0032496	44	0.000554505	response to lipopolysaccharide
BP	0002237	44	0.000697549	response to molecule of bacterial origin
BP	0051591	20	0.000697549	response to cAMP
BP	0022604	53	0.003299566	regulation of cell morphogenesis
BP	0050804	49	0.003299566	modulation of chemical synaptic transmission
BP	0099177	49	0.003299566	regulation of trans-synaptic signaling
BP	0007265	49	0.005501231	Ras protein signal transduction
BP	0061614	12	0.005501231	pri-miRNA transcription by RNA polymerase II
BP	0071674	17	0.005938402	mononuclear cell migration
BP	1902893	11	0.006251608	regulation of pri-miRNA transcription by RNA polymerase II
BP	0048008	13	0.006450711	platelet-derived growth factor receptor signaling pathway
BP	0050769	50	0.007151534	positive regulation of neurogenesis
BP	0032102	44	0.007609564	negative regulation of response to external stimulus
BP	0033673	32	0.008387946	negative regulation of kinase activity
BP	0042326	49	0.008387946	negative regulation of phosphorylation
BP	0043547	44	0.008387946	positive regulation of GTPase activity
BP	0007266	27	0.009405887	Rho protein signal transduction
BP	0051348	34	0.009405887	negative regulation of transferase activity
BP	0008360	22	0.009852937	regulation of cell shape
BP	1902895	9	0.009852937	positive regulation of pri-miRNA transcription by RNA polymerase II
BP	0070371	36	0.013673491	ERK1 and ERK2 cascade
BP	0051928	19	0.01448565	positive regulation of calcium ion transport
BP	0046683	20	0.014750353	response to organophosphorus
BP	0070372	34	0.019679851	regulation of ERK1 and ERK2 cascade

Ontology	ID(GO)	Count	*P*. adjust	Description
BP	0051056	37	0.019679851	regulation of small GTPase mediated signal transduction
BP	0071222	26	0.019679851	cellular response to lipopolysaccharide
BP	0048245	7	0.01982477	eosinophil chemotaxis
BP	0090280	7	0.01982477	positive regulation of calcium ion import
BP	0051017	21	0.025717384	actin filament bundle assembly
BP	0018205	41	0.025717384	peptidyl-lysine modification
BP	0043087	47	0.02778197	regulation of GTPase activity
BP	0071219	26	0.02778197	cellular response to molecule of bacterial origin
BP	0001933	43	0.031624154	negative regulation of protein phosphorylation
BP	0061572	21	0.031814019	actin filament bundle organization
BP	0035601	16	0.031814019	protein deacylation
BP	1901888	24	0.032450538	regulation of cell junction assembly
BP	0098732	16	0.033734125	macromolecule deacylation
BP	0050920	26	0.033992017	regulation of chemotaxis
BP	0002548	12	0.033992017	monocyte chemotaxis
BP	0009404	7	0.035579502	toxin metabolic process
BP	0014074	20	0.036265486	response to purine-containing compound
BP	0051271	39	0.037125299	negative regulation of cellular component movement
BP	0072677	7	0.042976418	eosinophil migration
BP	0007409	45	0.042976418	axonogenesis
BP	0006469	27	0.043536489	negative regulation of protein kinase activity
BP	0043405	35	0.044599144	regulation of MAP kinase activity
BP	0071216	27	0.044599144	cellular response to biotic stimulus
CC	0150034	41	1.50E-05	distal axon
CC	0099572	44	0.000104897	postsynaptic specialization
CC	0014069	41	0.000170875	postsynaptic density
CC	0032279	41	0.000176639	asymmetric synapse

Ontology	ID(GO)	Count	*P*. adjust	Description
CC	0030426	26	0.000377662	growth cone
CC	0030427	26	0.000523273	site of polarized growth
CC	0098984	41	0.000523273	neuron to neuron synapse
CC	0042641	15	0.002066292	actomyosin
CC	0098978	38	0.004457615	glutamatergic synapse
CC	0043025	49	0.004724047	neuronal cell body
CC	0005925	42	0.004724047	focal adhesion
CC	0030055	42	0.00634199	cell-substrate junction
CC	0000790	39	0.007035782	nuclear chromatin
CC	0010008	46	0.010610704	endosome membrane
CC	0044306	18	0.027781267	neuron projection terminus
CC	0099091	6	0.030243687	postsynaptic specialization, intracellular component
CC	0001725	11	0.037069496	stress fiber
CC	0097517	11	0.037069496	contractile actin filament bundle
CC	0031312	9	0.037069496	extrinsic component of organelle membrane
CC	0097060	40	0.037069496	synaptic membrane
CC	0000118	11	0.047793925	histone deacetylase complex
MF	0140297	50	1.02E-05	DNA-binding transcription factor binding
MF	0003714	32	0.005197605	transcription corepressor activity
MF	0001228	49	0.005197605	DNA-binding transcription activator activity, RNA polymerase II-specific
MF	0001216	49	0.005197605	DNA-binding transcription activator activity
MF	0031267	48	0.010060875	small GTPase binding
MF	0060589	39	0.015753176	nucleoside-triphosphatase regulator activity
MF	0061629	33	0.017728653	RNA polymerase II-specific DNA-binding transcription factor binding
MF	0017016	45	0.020961803	Ras GTPase binding
MF	0071889	8	0.020961803	14-3-3 protein binding

Ontology	ID(GO)	Count	P. adjust	Description
MF	0005096	32	0.020961803	GTPase activator activity
MF	0030695	34	0.029896089	GTPase regulator activity
MF	0008009	10	0.039151636	chemokine activity
MF	0030374	12	0.039151636	nuclear receptor transcription coactivator activity
MF	0004674	44	0.039151636	protein serine/threonine kinase activity
MF	0031434	5	0.039151636	mitogen-activated protein kinase kinase binding
MF	0030674	25	0.039151636	protein-macromolecule adaptor activity
MF	0048020	9	0.046447387	CCR chemokine receptor binding
MF	0017048	22	0.047317993	Rho GTPase binding
MF	0070491	12	0.047317993	repressing transcription factor binding

Then, KOBAS database and clusterProfiler package were used for KEGG enrichment analysis. The results showed that the DEGs were mainly enriched in Inflammation and cancer associated pathways (Fig. 4 & Table 2), including chemokine, IL-17, MAPK, TNF, NF-κB and Toll-like receptor signaling pathway. The bubble and bar diagram were plotted by the clusterProfiler package, and the length of the column and size of the circle represents the number of genes enriched in the pathway and their color stand for p value, which increases gradually from red to blue (Fig. 4. A-B). Also, the pathways with the most significant number of genes represented were showed as Fig. 4. C.

Table 2
Top10 pathway of KEGG analysis based on KAOBAS database

Term	ID	Input number	*P* value	Input
Metabolic pathways	hsa01100	10	0.0019	PLCB4、MAT2B、NT5E、CDO1、DMGDH、COX11、GPX8、ACADL、HIBCH、DERA
Chemokine signaling pathway	hsa04062	5	0.0001	CCL13、CCL1、PLCB4、RAP1A、GNAI1
Proteoglycans in cancer	hsa05205	5	0.0001	COL21A1、FZD2、IGF1、LUM、GPC3
Rap1 signaling pathway	hsa04015	5	0.0001	PDGFRA、IGF1、PLCB4、RAP1A、GNAI1
Pathways in cancer	hsa05200	5	0.0081	FZD2、IGF1、PLCB4、PDGFRA、GNAI1
Leukocyte transendothelial migration	hsa04670	4	0.0002	CLDN1、RAP1A、JAM2、GNAI1
Hippo signaling pathway	hsa04390	4	0.0005	SNAI2、BMPR1A、FZD2、FRMD6
Cushing syndrome	hsa04934	4	0.0005	FZD2、PLCB4、RAP1A、GNAI1
Long-term depression	hsa04730	3	0.0004	IGF1、PLCB4、GNAI1
Gap junction	hsa04540	3	0.0012	PDGFRA、PLCB4、GNAI1

3.5 Relationship between ENPP6 and biological pathways and functions

GSEA (version 4.0.3) was used for further enrichment analysis of GSEA-based GO and KEGG gene sets. The results showed that GO (Fig. 5. A) was enriched in protein localization, RNA splicing, autophagy and other related functions, and KEGG (Fig. 5. B) was enriched in IL-17 and TNF signaling pathway, etc., which basically consistent with the previous results. Also, we showed the GO results of the Top 10 significantly enriched in the bubble plots (Fig. 5. C).

We used the DEGs of two groups between high and low ENPP6 expression groups as the expression matrix, and 'c2.cp.v7.0.symbols.gmt' selected as the reference gene set for GSEA analysis with the standard thresholds *p* value < 0.05. RColorBrewer package were used for visualization of the GSEA results which showed that DEGs was enriched in ARF3 and P38/MK2 pathway in metabolism category of Pathway Interaction Database (PID), RHO and RAS pathway in BIOCARTA, and BRAFT and AKT1/E17K pathway in Reactome. And these pathways were significantly enriched in the ENPP6 low expression group (Fig. 5. D). These results indicated that the low expression of ENPP6 in with pain patients likely acted through above signaling pathways, and pain-mediated through indirect mechanisms such as a variety of cytokines and metabolic enzymes involved in the RAS and AKT pathway.

3.6 PPI network and key genes

We used the DEGs PPI networks which constructed by STRING database to predict protein-protein interactions (Fig. 6. A). Using the MCODE in Cytoscape to obtain the Hub genes, it shows the maximum correlation hub gene set, such as GNAI1, CCL1, CCL13 and P2RY14 (Fig. 6. B). Then, we obtained the bar chart of the Top 30 hub gene interactions using MCC analysis in cytoHubba (Fig. 6. C), and the length represents the number of molecular interactions. Next, we show the collection of hub genes obtained through using cytoHubba (Fig. 6. D), with darker colors representing higher related.

3.7 ENPP6 is correlated with autophagy phenotype and immunophenotype

A set of 2730 autophagy and immune related genes were obtained from HADb and ImmPort database. 231 DEGs were intersected with autophagy-related genes (232) and immune-related genes (2498) respectively, the result obtained 2 autophagy-related gene and 10 immune-related gene. Then, the Venn graph was generated using VennDiagram package. Subsequently, Pearson's correlation was used to analyze the correlations we analyzed the correlation between ENPP6 and 12 genes related to autophagy and immunophenotype, the phenotype related to differential gene and Pearson's correlation were listed in Table 3. Then, the highly score results were visualized using plot function in R software, displayed as correlation scatter plots (Fig. 7).

Table 3
Correlation analysis of ENPP6 with immune and
autophagy phenotypes

Relate gene	Phenotype	Pearson's correlation
GOPC	Autophagy	0.679
BNIP3L	Autophagy	0.653
IGF1	Immune	0.587
PDGFRL	Immune	0.752
CCL1	Immune	0.213
GNAI1	Immune	0.637
FAM3C	Immune	0.614
GNRH1	Immune	0.727
NRP1	Immune	0.749
PDGFRA	Immune	0.665
CCL13	Immune	0.598
BMPR1A	Immune	0.67

3.8 Relationship between ENPP6 and immune infiltrating

CIBERSORT package and LM22 algorithm were then used to analyze the abundance of 22 kinds of immune cells infiltration, including B cells, Plasma cells, T cells, NK cells and myeloid subsets, between the high and low ENPP6 expression groups in 16 with pain samples. As shown in the bar chart, each column represents one sample, each color represents one type of immune cell. From this, we can determine the infiltration abundance of each kind of immune cell in each sample (Fig. 8. A). Then we analyzed the expression differences of immune cells between the groups with high and low ENPP6 expression, and found that the activated NK cells were significantly highly expressed in the tissues with low ENPP6 expression, which was shown in the violin diagram (Fig. 8. B). Above results suggested that neuropathic pain may be closely related to inflammatory and metabolic pathways, and may change the proportion of immune cells distributed by predicting the targets small-molecule drugs of activated NK cells, thereby improving pain.

3.9 The diagnostic value of ENPP6 expression in with pain patients

In order to evaluate the diagnostic performance of ENPP6 for neuropathic pain, the pROC package was used to draw the receiver operating characteristic (ROC) curve to analyze whether the expression of

ENPP6 could distinguish between 5 non-pain samples and 16 pain samples, and determined the optimal cut-off value for generating the best likelihood ratio to determine the recognition threshold of ENPP6 for pain. The area under the curve (AUC) value was 0.925 (95% confidence interval [CI] = 0.8-1.0), indicating that the expression of ENPP6 can be of great value in diagnostic in neuropathic pain (Fig. 8. C).

3.10 The state of mutation in the ENPP family

Since the results suggested that ENPP6 was associated with the prognosis of NeP in cancer patients, the mutation status of this gene was analyzed furtherly. First, the list of ENPP family members, including ENPP1-7, were obtained from the HGNC database[31]. Then, the mutations of ENPP family members in 32 TCGA pan-cancer data sets was analyzed using the cBioPortal database. The results showed that mutation sites existed in ENPP 1−7 (Fig. 9. A). Subsequently, the mutations existing in 7 members of the ENPP family were presented, and the results showed that there were somatic, phosphorylation and endonuclease mutation sites of ENPP3, ENPP4 and ENPP5, while most of the mutations in ENPP4, ENPP5, ENPP6 and ENPP7 were phosphorylation sites (Fig. 9. B).

4 Discussion

Cancer-related neuropathic pain (NeP) is a common cause of chronic pain, which is one of the most difficult clinical problems[1, 2]. Despite an increasing number of available diagnosis and therapies, adequately diagnosis of NeP is often difficult and satisfactory pain control is not always achieved[2, 6, 7]. Therefore, novel molecular network biomarkers or targets are needed for earlier detection or treatment.

In the present study, we collected malignant tumors of the spine data based on RNA sequencing from published datasets, and demonstrated ENPP6 was significantly down-regulated in with pain samples compared with no pain samples. There are few reports on the expression of ENPP6 in cancer, while Yano Y et al. demonstrated that ENPP3 which is the same family as ENPP6 was expressed in the tumor cells of bile duct malignancies and may play a role in tumor infiltration[32]. And ENPP2 was expressed in thyroid cancer cells and may associated with tumor cell motility and tumorigenic capacity[33]. Then, we analyzed the function of ENPP6 in malignant tumors of the spine using GSEA, and the results indicated that the low expression of ENPP6 in with pain tissue may mediate pain through indirect mechanisms such as a variety of cytokines and metabolic enzymes involved in the RAS and AKT pathway. There is evidence indicates that Ras-AKT signaling can promote the progression of glioma[34]. Further analysis using the HPA database showed high expression of ENPP6 in normal brain tissue and low expression in brain tumor tissue (glioma)[35], which consistent with the foregoing results. Above evidence suggested that ENPP6 may be related to cancer and was differentially expressed in cancer.

Subsequently, using GO and KEGG pathway analysis, we found that DEGs was mostly enriched in the immunoinflammation-related and regulation of trans-synaptic signaling GO terms, and Inflammation and cancer associated pathways. Accumulating evidence shows that inflammation involved in the development of NeP. It has been demonstrated that ENPP6 is expressed in oligodendrocytes which necessary for transmission of bioelectrical signals and the protection of the normal function of

neurons[36]. In addition, ENPP2 have been revealed may play an important role in neural and vascular development, tumour progression and metastasis, as well as inflammation, neuropathic pain and fibrotic disease[37]. Xiao L et al have reported that ENPP6 may play a role in lipid metabolism during myelin sheath formation and might be required to initiate myelination rapidly in response to differentiation induced signals[36]. ENPP6, ENPP2 and ENPP7 shared recognition of phospholipids with choline. Evidence supported that ENPP7 is associated with anti-inflammatory and anti-tumorigenic activity by affecting the conversion of sphingomyelin to ceramide[38, 39]. Through these data, we found that ENPP6 may be involved in lipid metabolism, inflammation, cancer or nerve signaling, which prompted us to further analyze.

Afterward, the results of CIBERSORT analysis for the proportion of tumor-infiltrating immune cell (TIC) revealed that the expression of ENPP6 was positively correlated with immunophenotype and autophagy phenotype in spinal tumors patients. Then, we analyzed the expression differences of immune cells between the groups with high and low ENPP6 expression, and found that the activated NK cells were significantly highly expressed in the tissues with low ENPP6 expression. Natural Killer (NK) cells are lymphocytes with the capacity to target tumor cells via innate and adaptive responses[40, 41]. Activated NK cells can rapidly produce cytokines and activate other leukocytes, resulting increased complex fluctuations of cytokines observed in the blood and cerebrospinal fluid of NeP[42, 43]. Immune effector cells, especially NK cells, are associated with NeP[44]. Gao YH et al. reported that electroacupuncture improved NeP by affecting the activity and number of NK cells[45]. Morphine can inhibit the cytotoxic activity of NK cells through opioid receptors and Toll-like receptor-4 (TLR4), which is of great significance for the maintenance of immune function during pain[46]. Therefore, it is tempting to speculate that drugs targeted in activated NK cell may improve the proportion of immune cell distribution, and alleviate pain subsequently.

Furthermore, by analyzing the area under the ROC curve (AUC), we surprisingly found that ENPP6 had a good performance in diagnosing NeP. Recent reports indicated that choline plays a role in NeP and neuroinflammatory disorders[47, 48], and the role of ENPP6 in supplying choline to the cells have been well demonstrated[11]. Then, we analyzed the mutation status of the ENPP family, and the results showed that there were most of the mutations in ENPP4-7 were phosphorylation sites. Molecular and channel phosphorylation can affect the pathophysiological processes of NeP[49, 50]. García G et al reported that with mutations at PKC/PKA phosphorylation sites reversed tactile allodynia in neuropathic rats[51]. These suggested that the mutation of ENPP6 phosphorylation site may be one of the pathogenic links.

There are some limitations of our study. Firstly, the current study was only based on data analysis and additional experiments are needed to demonstrate the biological impact of ENPP6 in NeP. Secondly, the sample size of the data involved was small, and the study failed to cover different regions, which may affect the gene expression in tumors. Thirdly, because our study only focused on those genes that showed significant changes in the data set, some biological information might be ignored in our study. Therefore, further studies about direct mechanisms in NeP are needed.

In conclusion, this is the first study that uncovers ENPP6 may had a good performance in diagnosing NeP and may had an important role in the regulation of inflammatory and cancer pathways in malignant spinal tumors. The present study may offer new ideas for diagnosis and treatment of malignant spinal tumour patients with NeP.

Declarations

Ethical approvaland consent to participate

This study does not contain any studies with human participants or animals performed by any of the authors.

Consent for publication

All the authors have reviewed the final version of the manuscript and approved it for publication.

Availability of data and material

All data analyzed or generated are included in this article.

Competing interests

The authors declare that they have no competing interests.

Fundings

Authors' Contributions

J.H. performed analysis, and prepared the article. B.Z. supervised the analysis. Y.G. conceptualized the study design, provided supervision of the analysis and prepared the article.

Acknowledgements

References

1. Campbell JN, Meyer RA: **Mechanisms of neuropathic pain**. *Neuron* 2006, **52**(1):77-92.

2. Davis MP: **Cancer-Related Neuropathic Pain: Review and Selective Topics**. *Hematology/oncology clinics of North America* 2018, **32**(3):417-431.

3. Yamaoka S, Oshima Y, Horiuchi H, Morino T, Hino M, Miura H, Ogata T: **Altered Gene Expression of RNF34 and PACAP Possibly Involved in Mechanism of Exercise-Induced Analgesia for Neuropathic Pain in Rats**. *International journal of molecular sciences* 2017, **18**(9).

4. Schaub SK, Tseng YD, Chang EL, Sahgal A, Saigal R, Hofstetter CP, Foote M, Ko AL, Yuh WTC, Mossa-Basha M *et al*: **Strategies to Mitigate Toxicities From Stereotactic Body Radiation Therapy for Spine Metastases**. *Neurosurgery* 2019, **85**(6):729-740.

5. Bartels RH, van der Linden YM, van der Graaf WT: **Spinal extradural metastasis: review of current treatment options**. *CA: a cancer journal for clinicians* 2008, **58**(4):245-259.

6. Laufer I, Bilsky MH: **Advances in the treatment of metastatic spine tumors: the future is not what it used to be**. *Journal of neurosurgery Spine* 2019, **30**(3):299-307.

7. Sayari AJ, Pardo C, Basques BA, Colman MW: **Review of robotic-assisted surgery: what the future looks like through a spine oncology lens**. *Annals of translational medicine* 2019, **7**(10):224.

8. Coleman RE: **Clinical features of metastatic bone disease and risk of skeletal morbidity**. *Clinical cancer research : an official journal of the American Association for Cancer Research* 2006, **12**(20 Pt 2):6243s-6249s.

9. Stefan C, Jansen S, Bollen M: **NPP-type ectophosphodiesterases: unity in diversity**. *Trends in biochemical sciences* 2005, **30**(10):542-550.

10. Möller S, Jung C, Adriouch S, Dubberke G, Seyfried F, Seman M, Haag F, Koch-Nolte F: **Monitoring the expression of purinoceptors and nucleotide-metabolizing ecto-enzymes with antibodies directed against proteins in native conformation**. *Purinergic signalling* 2007, **3**(4):359-366.

11. Sakagami H, Aoki J, Natori Y, Nishikawa K, Kakehi Y, Natori Y, Arai H: **Biochemical and molecular characterization of a novel choline-specific glycerophosphodiester phosphodiesterase belonging to the nucleotide pyrophosphatase/phosphodiesterase family**. *The Journal of biological chemistry* 2005, **280**(24):23084-23093.

12. Mallat Z, Lambeau G, Tedgui A: **Lipoprotein-associated and secreted phospholipases A₂ in cardiovascular disease: roles as biological effectors and biomarkers**. *Circulation* 2010, **122**(21):2183-2200.

13. Morita J, Kano K, Kato K, Takita H, Sakagami H, Yamamoto Y, Mihara E, Ueda H, Sato T, Tokuyama H *et al*: **Structure and biological function of ENPP6, a choline-specific glycerophosphodiester-phosphodiesterase**. *Scientific reports* 2016, **6**:20995.

14. Fagerberg L, Hallström BM, Oksvold P, Kampf C, Djureinovic D, Odeberg J, Habuka M, Tahmasebpoor S, Danielsson A, Edlund K *et al*: **Analysis of the human tissue-specific expression by genome-wide integration of transcriptomics and antibody-based proteomics**. *Molecular & cellular proteomics : MCP* 2014, **13**(2):397-406.

15. Paic F, Igwe JC, Nori R, Kronenberg MS, Franceschetti T, Harrington P, Kuo L, Shin DG, Rowe DW, Harris SE *et al*: **Identification of differentially expressed genes between osteoblasts and osteocytes.**

Bone 2009, **45**(4):682-692.

16. Martin A, Quarles LD: **Evidence for FGF23 involvement in a bone-kidney axis regulating bone mineralization and systemic phosphate and vitamin D homeostasis**. *Advances in experimental medicine and biology* 2012, **728**:65-83.

17. Dawson G: **Measuring brain lipids**. *Biochimica et biophysica acta* 2015, **1851**(8):1026-1039.

18. Winter JM, Gildea DE, Andreas JP, Gatti DM, Williams KA, Lee M, Hu Y, Zhang S, Mullikin JC, Wolfsberg TG *et al*: **Mapping Complex Traits in a Diversity Outbred F1 Mouse Population Identifies Germline Modifiers of Metastasis in Human Prostate Cancer**. *Cell systems* 2017, **4**(1):31-45.e36.

19. van Hecke O, Austin SK, Khan RA, Smith BH, Torrance N: **Neuropathic pain in the general population: a systematic review of epidemiological studies**. *Pain* 2014, **155**(4):654-662.

20. Hill R: **NK1 (substance P) receptor antagonists--why are they not analgesic in humans?** *Trends in pharmacological sciences* 2000, **21**(7):244-246.

21. North RY, Li Y, Ray P, Rhines LD, Tatsui CE, Rao G, Johansson CA, Zhang H, Kim YH, Zhang B *et al*: **Electrophysiological and transcriptomic correlates of neuropathic pain in human dorsal root ganglion neurons**. *Brain : a journal of neurology* 2019, **142**(5):1215-1226.

22. Anders S, Huber W: **Differential expression analysis for sequence count data**. *Genome biology* 2010, **11**(10):R106.

23. Ritchie ME, Phipson B, Wu D, Hu Y, Law CW, Shi W, Smyth GK: **limma powers differential expression analyses for RNA-sequencing and microarray studies**. *Nucleic acids research* 2015, **43**(7):e47.

24. Huang da W, Sherman BT, Lempicki RA: **Bioinformatics enrichment tools: paths toward the comprehensive functional analysis of large gene lists**. *Nucleic acids research* 2009, **37**(1):1-13.

25. Huang DW, Sherman BT, Tan Q, Kir J, Liu D, Bryant D, Guo Y, Stephens R, Baseler MW, Lane HC *et al*: **DAVID Bioinformatics Resources: expanded annotation database and novel algorithms to better extract biology from large gene lists**. *Nucleic acids research* 2007, **35**(Web Server issue):W169-175.

26. Yu G, Wang LG, Han Y, He QY: **clusterProfiler: an R package for comparing biological themes among gene clusters**. *Omics : a journal of integrative biology* 2012, **16**(5):284-287.

27. Subramanian A, Kuehn H, Gould J, Tamayo P, Mesirov JP: **GSEA-P: a desktop application for Gene Set Enrichment Analysis**. *Bioinformatics (Oxford, England)* 2007, **23**(23):3251-3253.

28. Szklarczyk D, Gable AL, Lyon D, Junge A, Wyder S, Huerta-Cepas J, Simonovic M, Doncheva NT, Morris JH, Bork P *et al*: **STRING v11: protein-protein association networks with increased coverage, supporting functional discovery in genome-wide experimental datasets**. *Nucleic acids research* 2019, **47**(D1):D607-d613.

29. Newman AM, Liu CL, Green MR, Gentles AJ, Feng W, Xu Y, Hoang CD, Diehn M, Alizadeh AA: **Robust enumeration of cell subsets from tissue expression profiles**. *Nature methods* 2015, **12**(5):453-457.

30. Braschi B, Denny P, Gray K, Jones T, Seal R, Tweedie S, Yates B, Bruford E: **Genenames.org: the HGNC and VGNC resources in 2019**. *Nucleic acids research* 2019, **47**(D1):D786-d792.

31. Massé K, Bhamra S, Allsop G, Dale N, Jones EA: **Ectophosphodiesterase/nucleotide phosphohydrolase (Enpp) nucleotidases: cloning, conservation and developmental restriction**. *The International journal of developmental biology* 2010, **54**(1):181-193.

32. Yano Y, Hayashi Y, Sano K, Nagano H, Nakaji M, Seo Y, Ninomiya T, Yoon S, Yokozaki H, Kasuga M: **Expression and localization of ecto-nucleotide pyrophosphatase/phosphodiesterase I-1 (E-NPP1/PC-1) and -3 (E-NPP3/CD203c/PD-Ibeta/B10/gp130(RB13-6)) in inflammatory and neoplastic bile duct diseases**. *Cancer letters* 2004, **207**(2):139-147.

33. Seifert A, Klonisch T, Wulfaenger J, Haag F, Dralle H, Langner J, Hoang-Vu C, Kehlen A: **The cellular localization of autotaxin impacts on its biological functions in human thyroid carcinoma cells**. *Oncology reports* 2008, **19**(6):1485-1491.

34. Sang B, Sun J, Yang D, Xu Z, Wei Y: **Ras-AKT signaling represses the phosphorylation of histone H1.5 at threonine 10 via GSK3 to promote the progression of glioma**. *Artificial cells, nanomedicine, and biotechnology* 2019, **47**(1):2882-2890.

35. Uhlén M, Fagerberg L, Hallström BM, Lindskog C, Oksvold P, Mardinoglu A, Sivertsson Å, Kampf C, Sjöstedt E, Asplund A *et al*: **Proteomics. Tissue-based map of the human proteome**. *Science (New York, NY)* 2015, **347**(6220):1260419.

36. Xiao L, Ohayon D, McKenzie IA, Sinclair-Wilson A, Wright JL, Fudge AD, Emery B, Li H, Richardson WD: **Rapid production of new oligodendrocytes is required in the earliest stages of motor-skill learning**. *Nature neuroscience* 2016, **19**(9):1210-1217.

37. Hausmann J, Kamtekar S, Christodoulou E, Day JE, Wu T, Fulkerson Z, Albers HM, van Meeteren LA, Houben AJ, van Zeijl L *et al*: **Structural basis of substrate discrimination and integrin binding by autotaxin**. *Nature structural & molecular biology* 2011, **18**(2):198-204.

38. Duan RD, Nilsson A: **Metabolism of sphingolipids in the gut and its relation to inflammation and cancer development**. *Progress in lipid research* 2009, **48**(1):62-72.

39. Cheng Y, Wu J, Hertervig E, Lindgren S, Duan D, Nilsson A, Duan RD: **Identification of aberrant forms of alkaline sphingomyelinase (NPP7) associated with human liver tumorigenesis**. *British journal of cancer* 2007, **97**(10):1441-1448.

40. Wiedemann GM, Grassmann S, Lau CM, Rapp M, Villarino AV, Friedrich C, Gasteiger G, O'Shea JJ, Sun JC: **Divergent Role for STAT5 in the Adaptive Responses of Natural Killer Cells**. *Cell reports* 2020, **33**(11):108498.

41. Javed A, Milhem M: **Role of Natural Killer Cells in Uveal Melanoma**. *Cancers* 2020, **12**(12).

42. Alexander GM, van Rijn MA, van Hilten JJ, Perreault MJ, Schwartzman RJ: **Changes in cerebrospinal fluid levels of pro-inflammatory cytokines in CRPS**. *Pain* 2005, **116**(3):213-219.

43. Khoonsari PE, Ossipova E, Lengqvist J, Svensson CI, Kosek E, Kadetoff D, Jakobsson PJ, Kultima K, Lampa J: **The human CSF pain proteome**. *Journal of proteomics* 2019, **190**:67-76.

44. Davies AJ, Rinaldi S, Costigan M, Oh SB: **Cytotoxic Immunity in Peripheral Nerve Injury and Pain**. *Frontiers in neuroscience* 2020, **14**:142.

45. Gao YH, Wang JY, Qiao LN, Chen SP, Tan LH, Xu QL, Liu JL: **NK cells mediate the cumulative analgesic effect of electroacupuncture in a rat model of neuropathic pain**. *BMC complementary and alternative medicine* 2014, **14**:316.

46. Maher DP, Walia D, Heller NM: **Morphine decreases the function of primary human natural killer cells by both TLR4 and opioid receptor signaling**. *Brain, behavior, and immunity* 2020, **83**:298-302.

47. Chang L, Munsaka SM, Kraft-Terry S, Ernst T: **Magnetic resonance spectroscopy to assess neuroinflammation and neuropathic pain**. *Journal of neuroimmune pharmacology : the official journal of the Society on NeuroImmune Pharmacology* 2013, **8**(3):576-593.

48. Petho G, Reeh PW: **Sensory and signaling mechanisms of bradykinin, eicosanoids, platelet-activating factor, and nitric oxide in peripheral nociceptors**. *Physiological reviews* 2012, **92**(4):1699-1775.

49. Blesneac I, Chemin J, Bidaud I, Huc-Brandt S, Vandermoere F, Lory P: **Phosphorylation of the Cav3.2 T-type calcium channel directly regulates its gating properties**. *Proceedings of the National Academy of Sciences of the United States of America* 2015, **112**(44):13705-13710.

50. Gomez K, Calderón-Rivera A, Sandoval A, González-Ramírez R, Vargas-Parada A, Ojeda-Alonso J, Granados-Soto V, Delgado-Lezama R, Felix R: **Cdk5-Dependent Phosphorylation of Ca(V)3.2 T-Type Channels: Possible Role in Nerve Ligation-Induced Neuropathic Allodynia and the Compound Action Potential in Primary Afferent C Fibers**. *The Journal of neuroscience : the official journal of the Society for Neuroscience* 2020, **40**(2):283-296.

51. García G, Méndez-Reséndiz KA, Oviedo N, Murbartián J: **PKC- and PKA-dependent phosphorylation modulates TREK-1 function in naïve and neuropathic rats**. *Journal of neurochemistry* 2020.
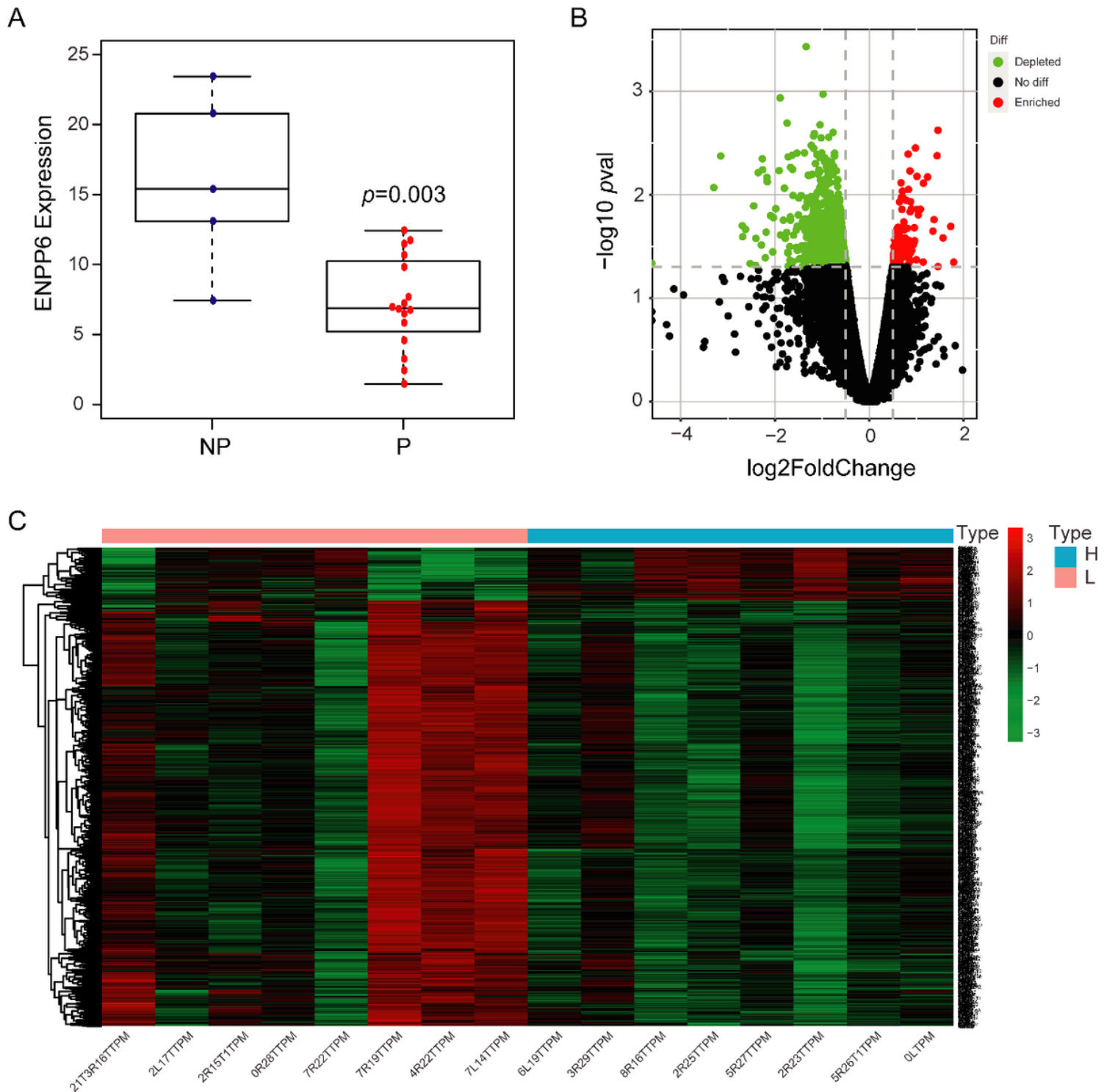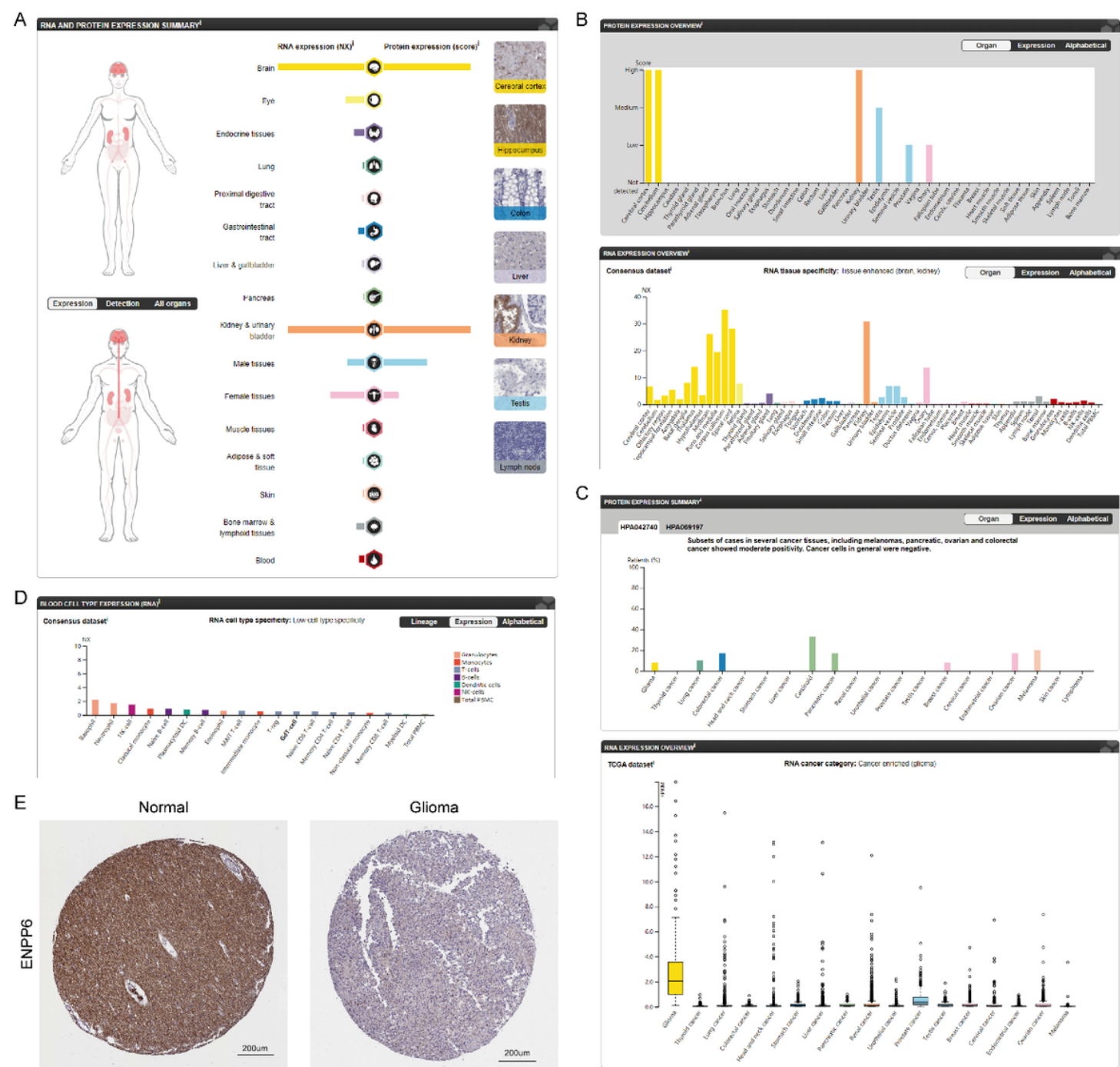
Figures

Figure 1

ENPP6 and co-expression gene differential analysis. (A) Differential expression of ENPP6 in NP group (n = 5 samples) vs P group (n = 16 samples). (B) Volcano plots for DEGs between NP and P group. Normalized expression levels are shown in descending order from red to green. (C) Heatmap for co-expression gene associated with the expression level of ENPP6. According to expression of ENPP6, the DRG samples of 16 patients with pain were divided into high (H, n = 6 samples) and low (L, n = 6 samples) expression groups. The column and row represented the samples and genes, respectively.

Green and red tones represent downregulated and upregulated genes. P, with pain samples; NP, no pain samples; DEGs, differentially expressed genes; H, ENPP6 high expression group; L, ENPP6 low expression group.

Figure 2

Expression of ENPP6 in normal and tumor tissues. (A) ENPP6 expression in human different tissues. Protein and mRNA expression of ENPP6 in normal brain tissue (B) and gliomas (C). (D) Expression of ENPP6 in different types of blood cells. (E) Immunohistochemical staining of ENPP6 in normal brain tissues and glioma.

Figure 3

Gene Ontology (GO) enrichment analysis. GO enrichment bar chart (A) and bubble plots (B) of upregulated genes (DEG) representing the number of DEGs enriched in biological process, cellular component and molecular function. The length of the column and size of the circle represents the number of genes enriched in the pathway and their color stand for p value, which increases gradually from red to blue. The GO enrichment analysis network was constructed by Bingo (C) and ClueGO (D) in

Cytoscape. Each dot represents a GO term, of which their size stand for the correlation of DEGs, which increases gradually from smaller to bigger. (C) The color stand for p value, which increases gradually from dark to light. (D) The color represents the degree of DEGs enrichment. BP, biological process; CC, cellular component; MF, molecular function.
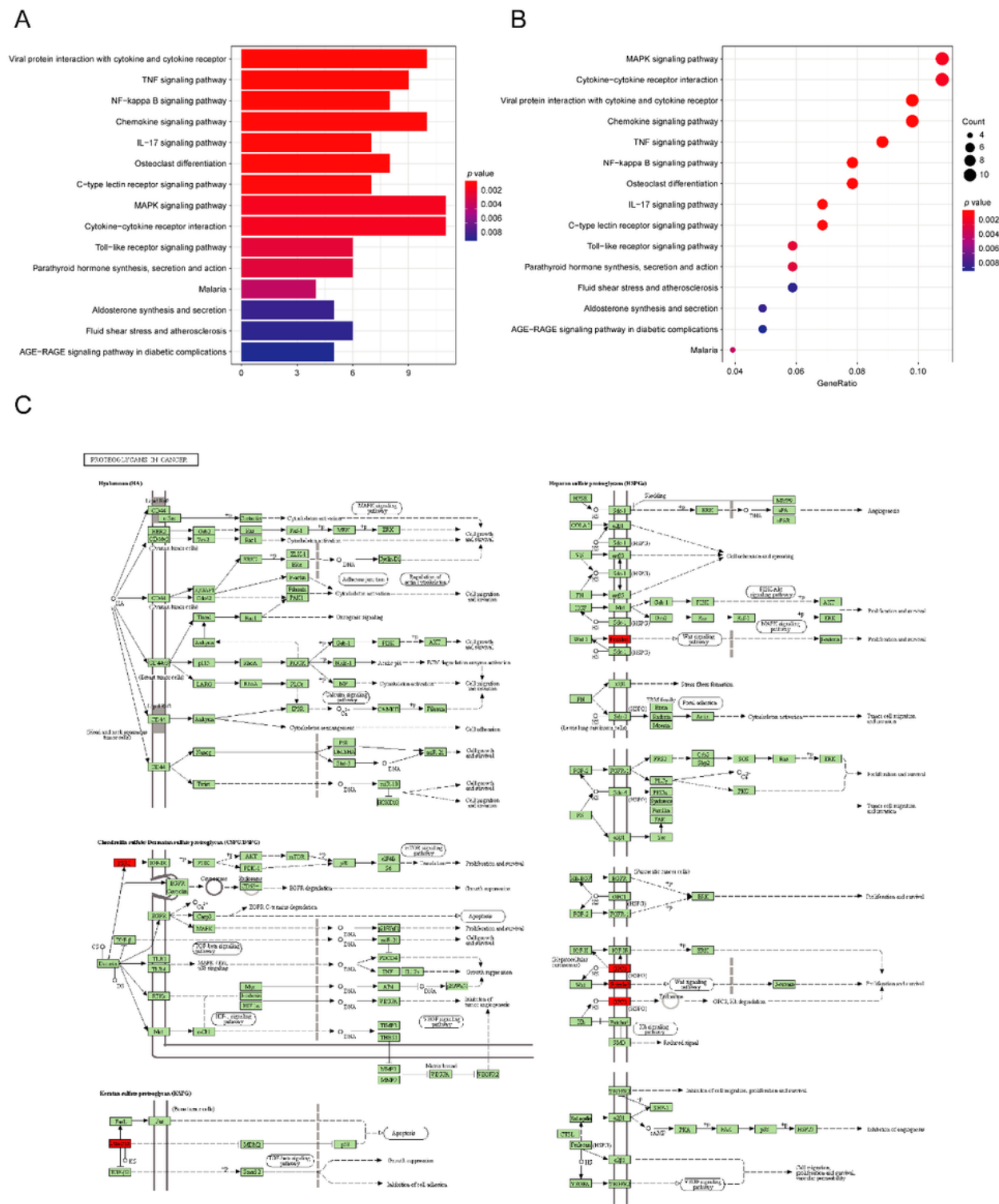
Figure 4

Kyoto Encyclopedia of genes and genomes (KEGG) enrichment analysis. KEGG enrichment bar chart (A) and bubble plots (B) representing the number of DEGs enriched in related pathways. The length of the column and size of the circle represents the number of genes enriched in the pathway and their color stand for p value, which increases gradually from red to blue. (C) KEGG pathway annotations of proteoglycans in cancer.
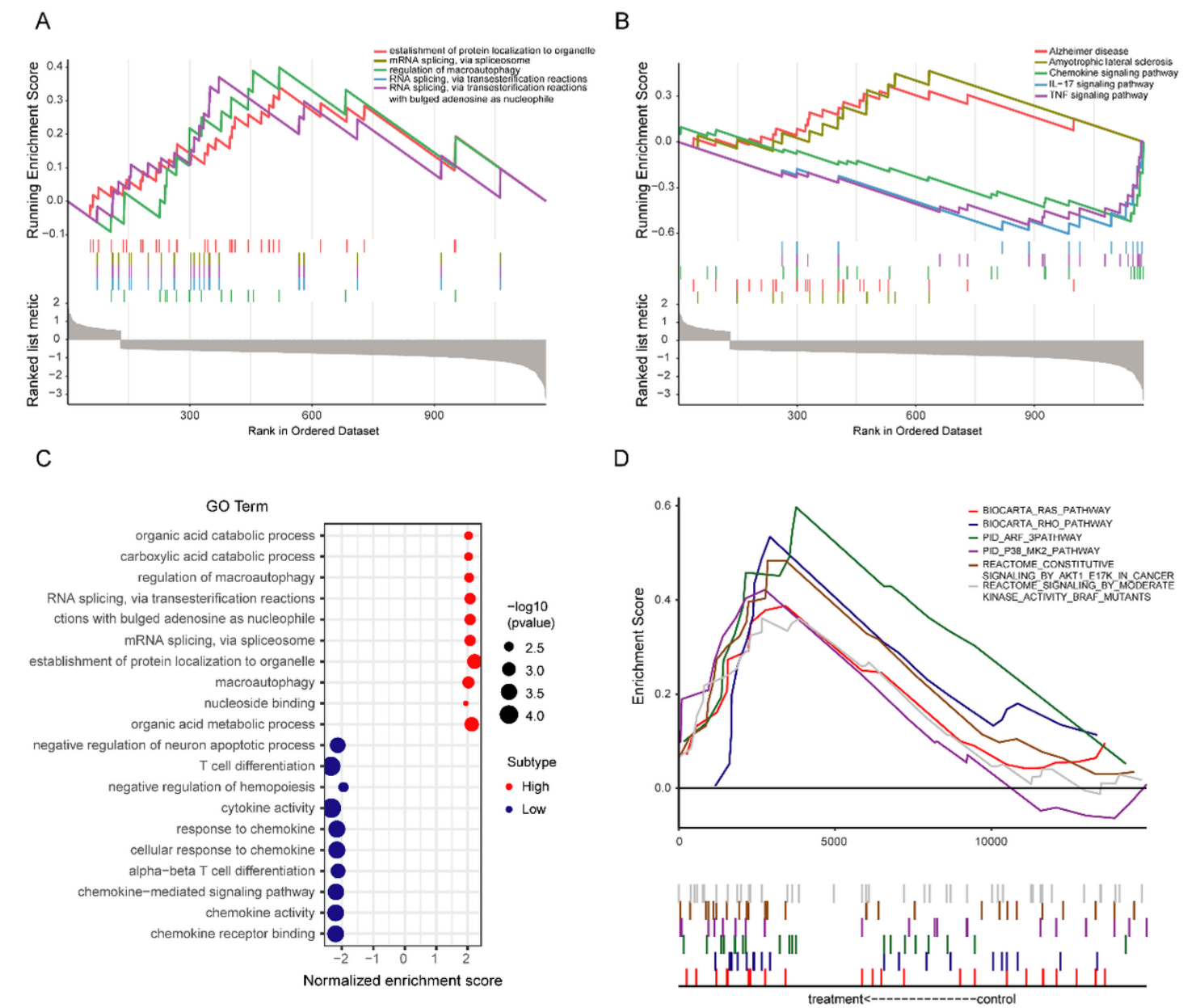
Figure 5

Gene-set enrichment analysis (GSEA) enrichment analysis. (A) GSEA-based GO-enrichment plots of representative gene sets. (B) GSEA-based KEGG-enrichment plots of representative gene sets. Each line with different color representing a pathway, with up-regulated genes located in the left, while down-regulated in the right of the x-axis. Only several main pathways were showed in the plot. (C) Functional enrichment analysis (GO results) of top 10 gene in ENPP6 high and low expression groups. (D) Pathways

with significant enrichment of DEG in the ENPP6 high and low expression groups: RAS, RHO, ARF3, P38/MK2, AKT1/E17K, BRAFT.
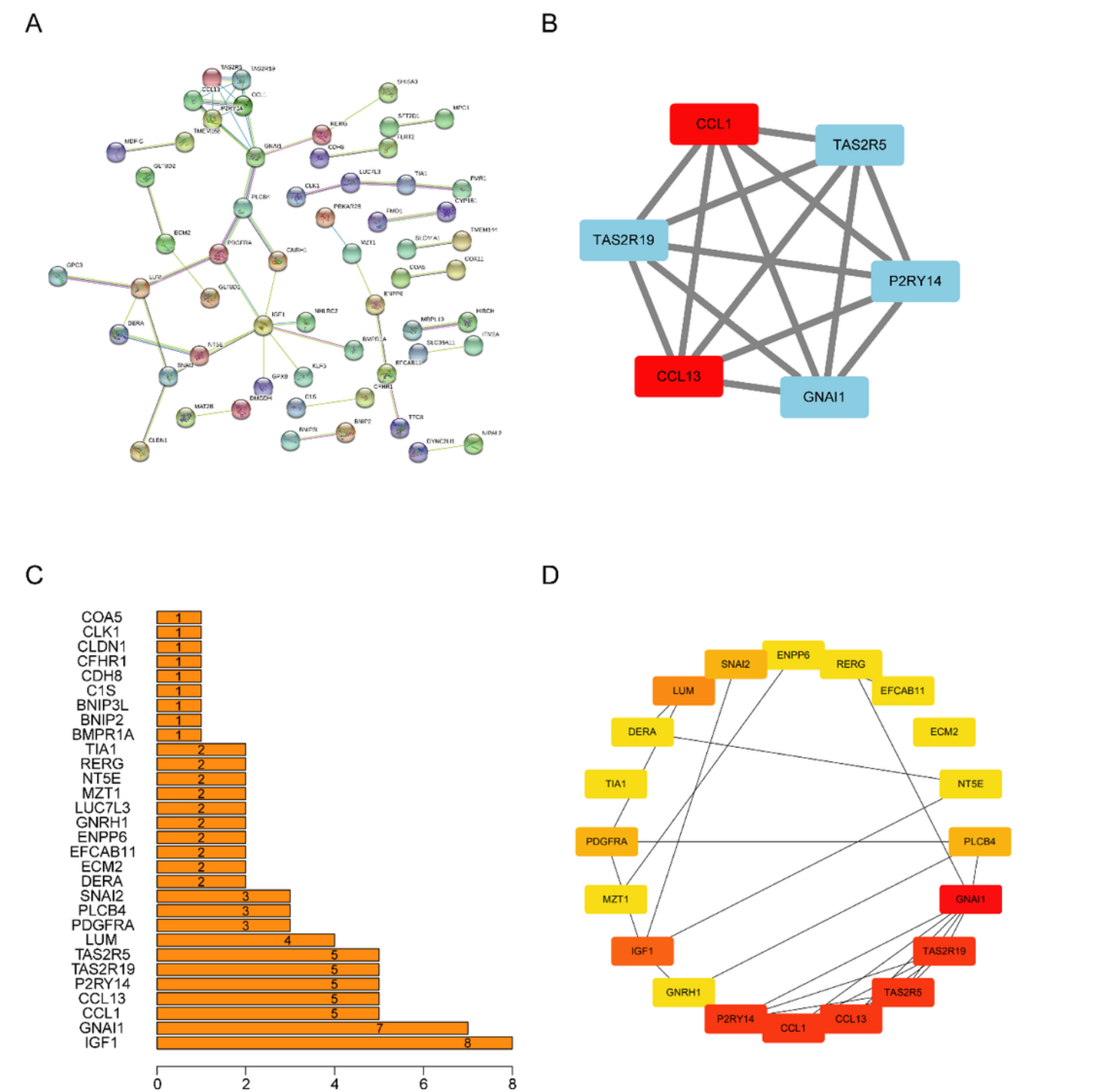

Figure 6

Protein-protein interaction (PPI) network. (A) The PPI constructed with the interaction score was set to confidence of 0.4. (B) The MCODE in Cytoscape was used to obtain the hub genes with maximum correlation criterion. (C) The cytoHubba in Cytoscape was used to obtain the bar chart of top 30 hub gene

interactions. The length represents the number of molecular interactions. (D) Hub genes set has been obtained and shown by cytoHubba in Cytoscape.
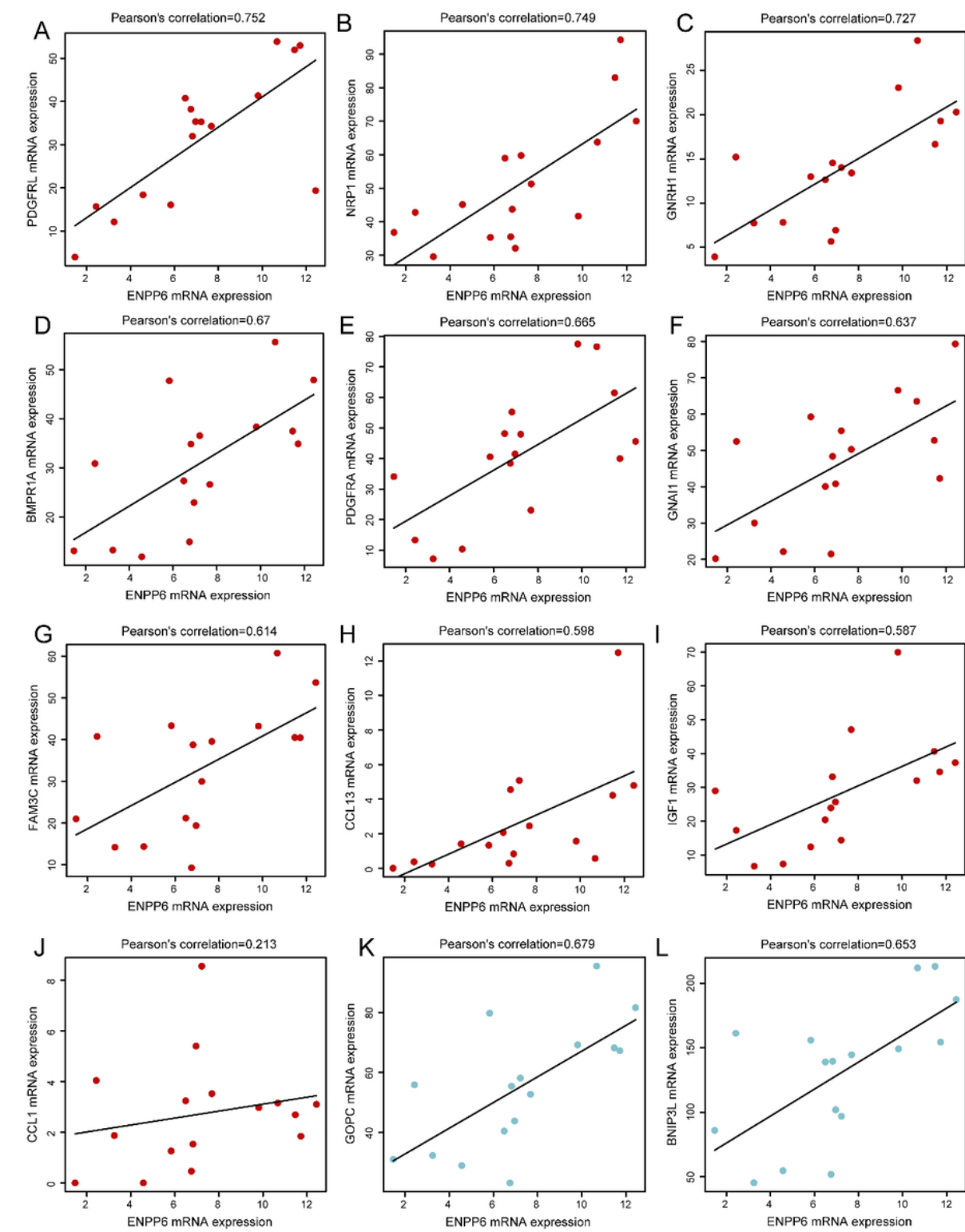

Figure 7

Phenotypic correlation analysis of ENPP6. (A-G) Scatter plot showing the of ENPP6 and immune-related phenotypic DEG. (H-L) Correlation of ENPP6 and autophagy-related phenotypic DEG. The line in each plot

was fitted linear model indicating the proportion tropism of the immune or autophagy related cell along with ENPP6 expression, and Pearson coefficient was used for the correlation test.
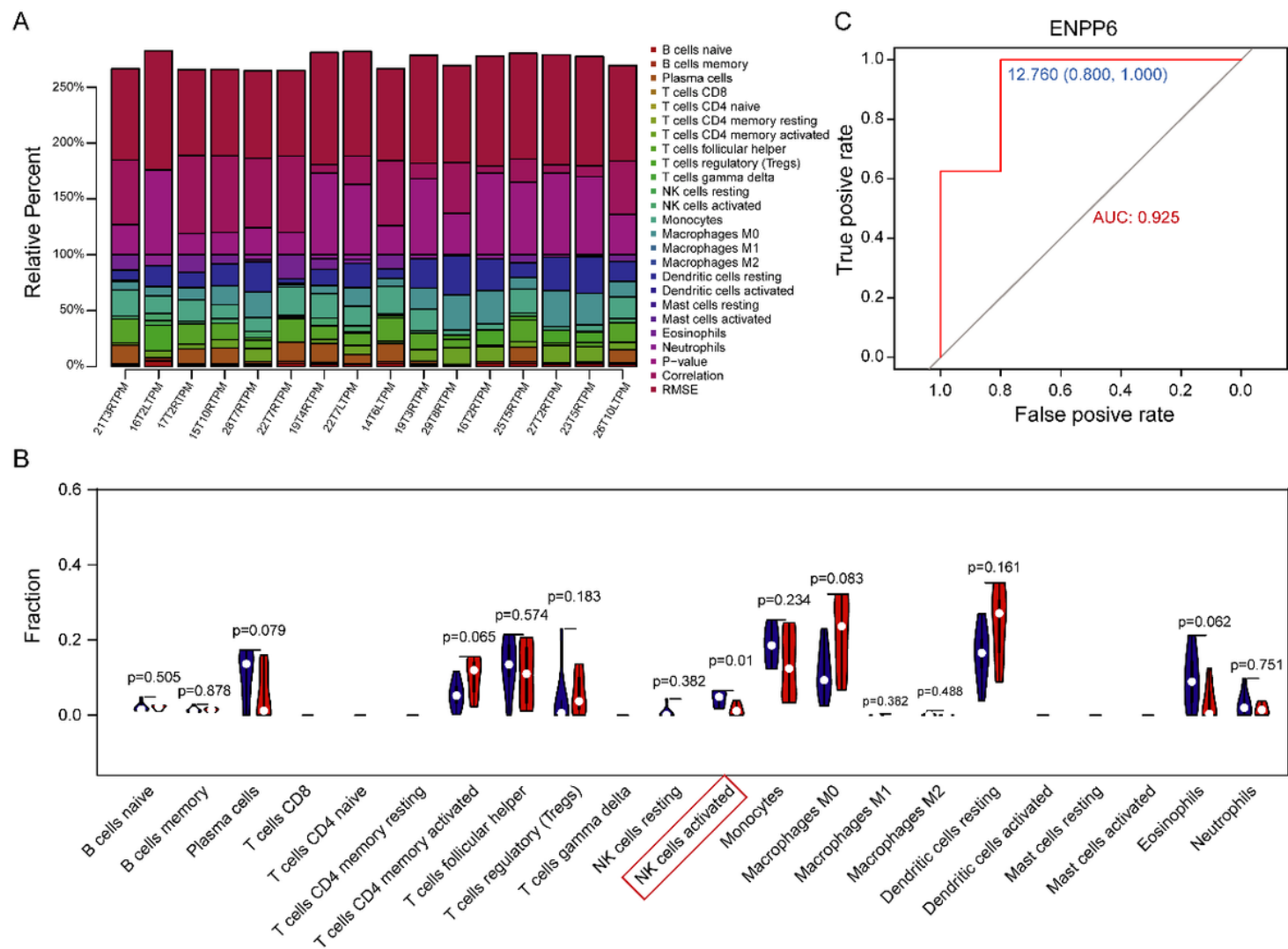

Figure 8

The abundance and expression difference of immunocompromised cells and the diagnostic performance of ENPP6. (A) Bar plot showing the proportion of 22 kinds of immune cell infiltrates between high and low ENPP6 expression groups in 16 pain samples. (B) Violin plot showing the ratio differentiation of 22 kinds of immune cells between 16 tumor samples with high and low ENPP6 expression relative to the median of ENPP6 expression level, and Wilcoxon rank sum was used for the significance test. Blue represents the low expression group, red represents the high expression group, p < 0.05 is considered to have significant difference. (C) Area under the ROC curve (AUC) evaluates the diagnostic performance of ENPP6 for pain.
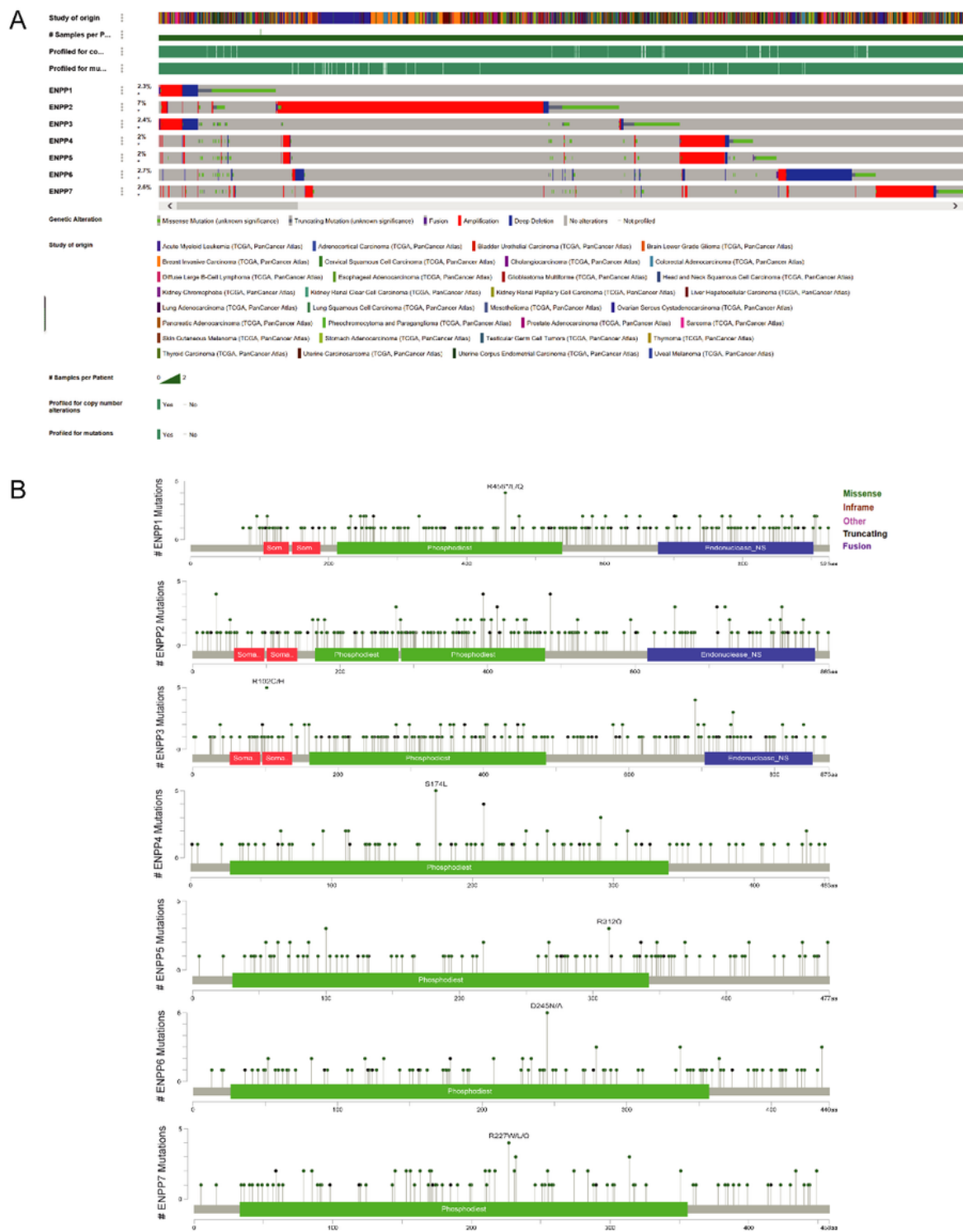
Figure 9

ENPP6 mutation analysis. (A) Mutations analysis of ENPP family members in 32 TCGA pan carcinoma datasets. (B) Mutations sites in members of the ENPP family.

Supplementary Files

This is a list of supplementary files associated with this preprint. Click to download.

- Supplementarymaterial.rar